Tc(VII)/Tc(V) direct coordination with secondary building unit of uranyl hybrid materials and their isolation as molecular cluster

Mohammad Shohel[a] and May Nyman*[a]

[a]*Department of Chemistry, Oregon State University, Corvallis, OR-97331, USA.*

**Corresponding author: may.nyman@oregonstate.edu*

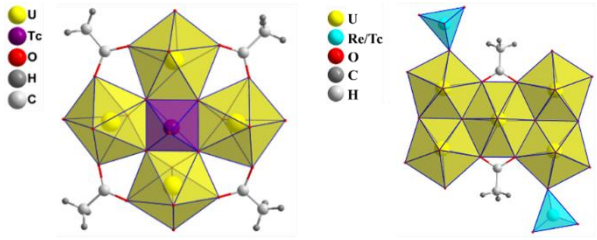

Tc-99 oxoanion pertechnetate (TcO_4^-), reduced Tc species and actinides co-exist in spent nuclear fuel/legacy waste and co-extract together during reprocessing. Herein, we reported five new molecular cluster/extended structures with pentameric/tetrameric uranyl building units directly coordinated to oxoanion TcO_4^-/ReO_4^- (surrogate) and reduced technetium cation Tc(V). The isolation and characterization of these new compounds will be useful in furthuring the understanding of coordination between Tc species and actinides, which is critical for their efficient seperation/recovery.

Technetium-99 (Tc-99) is one of the highest-yield and long-lived decay product of the U-235 fission reaction, utilized in nuclear energy and weapons. Technetium poses a challenge during solvent-extraction based reprocessing of spent nuclear fuel by co-extracting with actinides and other elements, hampering efficient separation[1]. One possible mechanism of this co-extraction process is coordination of pertechnetate (TcO_4^-) with actinides and other metal ions present in the spent nuclear fuel[2, 3]. However, there is limited isolation and structural characterization of compounds that directly evidence direct coordination of pertechnetate/perrhenate (ReO_4^-, a well-known surrogate for TcO_4^-) with actinides and other metals present in spent nuclear fuel as process chemicals or fission products (i.e. Zr).[4-8] By expanding the library of metal cation-pertechnetate/perrhenate coordination compounds, our fundamental knowledge of Tc behaviour in a range of relevant complex matrices will grow considerably.

One such complex matrix is legacy nuclear wastes stored in Hanford WA and the Savannah River site. Due to the persistency ($T_{1/2}$ = 2.11x10^5 y), radioactivity (β = 292 keV), variable redox states, and high mobility in the environment via solubility or volatilization (i.e. as Tc_2O_7), Tc-99 is one of the greatest challenges in nuclear waste management and disposal[9]. In the highly alkaline environments relevant to tank waste supernatants, Tc is expected to exist as the fully oxidized TcO_4^- (pertechnetate) species[10]. However, due to presence of organics, coupled with radiolysis and catalytic activity in tank waste, low valent/reduced Tc species have been also identified with percentage as high as 80% of total Tc[11, 12]. The speciation of low valent Tc and their chemical interaction with other species in tank waste, including actinides, is still not well-understood.

The hybrid materials can broadly be defined as a compound that contains both inorganic and organic components interacting on a molecular level[13]. Uranyl hybrid materials built of UO_2^{2+} plus organic or inorganic ligands and/or linkers have gained signifiant attention in last two decades. Motivation towards studying this system has arisen from the interest in uranyl metal organic frameworks (MOFs) and understanding transformation of U(VI) species from solution to solid state[14, 15]. The most studied system of uranyl hybrid materials is composed of Secondary Building Unit (SBU) made of U(VI) which are connected by organics to form an extended structure[16]. The SBUs in uranyl hybrid materials are also analogous to building units present in uranyl bearing minerals[17]. The topology of uranyl SBUs in hybrid materials/minerals varies from finite nodes (monomer, dimer, trimer, tetramer, etc.) to infinite chains and sheets, where the multiply-bound oxos of the linear uranyl unit have strong structure directing effects, favoring low-dimensional assemblies. Isolating the SBU building blocks as soluble molecular clusters (instead of infinite lattices) is challenging, as surmised from the paucity of published structures and solution phase studies.[4, 18, 19] Isolation and solution studies of SBUs can yield valuable information about assembly pathways of uranyl hybrid materials and minerals. The extended structures of SBUs have been synthesized using carboxylates, carboxyphosphonates, and halides, considering the prevalence of these functional groups in environmental, reprocessing, or potential long-term waste stewardship settings[16, 20-22]. In addition, different inorganic ions such as carbonate[23], phosphate[24-26], sulfate[27, 28], selenate[27] vanadate[19], molybdate[29], silicate[30] etc. are used as linkers for SBUs in order to develop uranyl solid state chemistry and understand in complex mineral topologies. Perrhenate, isostructural with the above-mentioned tetrahedral oxoanions, also has demonstrated uranyl-ligation in molecular forms with phosphonate heteroligands[31], in layered materials with

perrhenate linking uranyl into sheets, and isolated perrhenate-capped flat dimers and trimers[4]. Despite it's relevancy in spent nuclear fuel reprocessing and tank waste chemistry, there are no reported structures featuring coordination between uranyl and pertechnetate or reduced technetium.

Here we present five new uranyl compounds, where SBUs are directly coordinated to oxoanions TcO_4^-/ReO_4^- and the reduced technetium cation $Tc(V)O^{3+}$. Amongst those five compounds, three are molecular clusters that have a unique pentameric/tetrameric uranyl unit. The structures of the compounds have been elucidated from Single Crystal X-ray Diffraction (SCXRD). Bulk crystalline materials have also been characterized by Fourier Transform Infrared Spectroscopy (FTIR), Raman Spectroscopy, Powder X-ray Diffraction (PXRD) and Scanning Electron Microscopy-Energy Dispersive Spectroscopy (SEM-EDS). In addition, Small Angle X-ray Scattering (SAXS) of solutions has also been employed to study solution speciation.

The compounds have been synthesized from reaction between uranyl acetate and perrhenic/pertechnic acid solutions followed by crystallization through evaporation (more details in SI). The structures of the compounds contain liner axial uranyl cation (UO_2^{2+}) bonded with additional oxygen in equatorial sites to form either hexagonal or pentagonal bipyramidal geometry. The U-O bond distance in axial position ranges from 1.756(8)-1.792(5) Å and equatorial position ranges from 2.217(2)- 2.592(4) Å. The Re(VII)/Tc(VII) metal centre poses a tetrahedral geometry in the structure through ReO_4^- /TcO_4^- anions. The Re-O bond length ranges in between

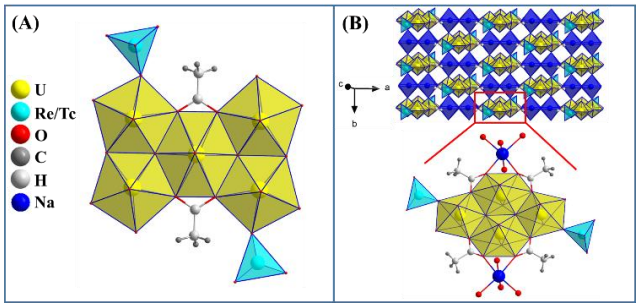

Figure 1. Polyhedral representation of **A**) U_5Re_2/U_5Tc_2 molecular cluster and (**B**) U_4Re_2/U_4Tc_2 2D framework and it's building block (inset).

1.709(5)-1.739(5) Å. On the other hand, the Tc-O bond length ranges in between 1.689(8)-1.732(7) Å. The SI contain details of SCXRD analysis and selected crystallographic information for the isolated structures (**Table S1**). The bond valence sum (BVS) calculation for different crystallographic sites in isolated structures are done (**Table S2**). The calculated average BVS values for fully occupied U(VI), Re(VII) and Tc(VII) sites were 6.06, 6.86 and 6.65, respectively. The bond distance and BVS value for Tc(V) site has been discussed later in the manuscript.

U_5Re_2 and U_5Tc_2 are unique analogous pentameric uranyl molecular cluster. The uranyl pentamer formed from edge sharing of four pentagonal uranyl bipyramids and a hexagonal uranyl bipyramid (**Figure 1A**). The uranyl pentamer is additionally coordinated by acetate and perrhenate/pertechnetate ions. The central hexagonal bipyramid is composed of a linear uranyl cation that is coordinated to two μ_3-oxo and four oxygen atoms from acetate. The two μ_3-oxos serve as a bridge to connect two pentagonal uranyl bipyramids dimers in each side, which are flanking the central hexagonal bipyramid. Other than μ3-oxo, the pentagonal uranyl bipyramids are also coordinated to oxygen atoms from μ_2-oxo, H_2O and acetate in their equatorial position. Two of the four pentagonal uranyl bipyramids are also coordinated to oxygen from perrhenate/pertechnetate. The overall molecular formula of the U_5Re_2 and U_5Tc_2 molecular cluster is: $[(UO_2)_5(O)_2(OH)_2(H_2O)_6(MO_4)_2(CH_3COO)_2]$, where M= Re/Tc. The packing of the clusters in extended crystal structure is depicted in **Figure S1**. The $(UO_2)_5$ pentamer building block was

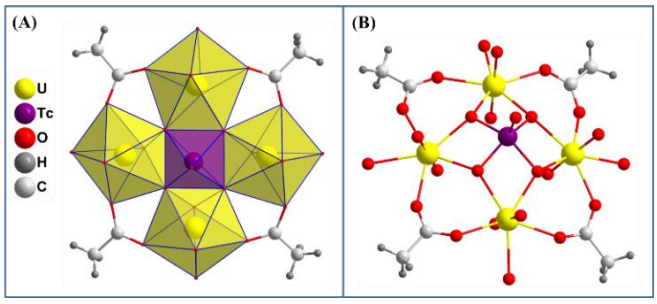

Figure 2. (**A**) Polyhedral representation of U_4Tc molecular cluster and (**B**) Ball-stick representation of U_4Tc molecular cluster.

part of extended uranyl hybrid materials that were synthesized with sulfobenzoate[32], phosphate[20] and phosphonoacetate[33]. However, U_5Re_2 and U_5Tc_2 are the first example of crystallizing $(UO_2)_5$ unit as molecular cluster.

U_4Re_2 and U_4Tc_2 are analogous 2D framework with presence of tetrameric uranyl cluster as building block. The tetramer formed by edge sharing of two hexagonal and two pentagonal uranyl bipyramids (**Figure 2B**). The two hexagonal uranyl bipyramids are connected with each other by two μ3-oxo, each of which are again connected to uranyl pentagonal bipyramid that flanked the hexagons. The uranyl pentagonal bipyramid are also coordinated to oxygens from acetate, H_2O and perrhenate/pertechnetate. On the other hand, hexagonal uranyl bipyramids are additionally coordinated by oxygens from acetate and NaO_6 unit. The overall molecular formula of the framework is: $[(UO_2)_4(O)_2(H_2O)_2(MO_4)_2(CH_3COO)_4Na_2(OH)_2]$, where M=Re/Tc. The NaO_6 unit connects the uranyl tetramer in the framework by bonding with neighboring NaO_6 unit through μ2-oxo. In the extended structure the 2D framework stack on top of each other along c axis (**Figure S2**). The uranyl tetramer $(UO_2)_4$ containing hybrid materials has been published before[34-36] including recent report of their isolation as molecular cluster by Felton *et al.* 2023[19].

U_4Tc is an unique pentameric molecular cluster composed of four uranyl pentagonal bipyramids and one $Tc(V)O_5$ "umbrella". $Tc(V)O_5$ umbrella composed of a Tc=O bond in axial position and four Tc-O bond in equatorial position. The U_4Tc formed from edge sharing of four individual uranyl pentagonal bipyramids with $Tc(V)O_5$ umbrella by equatorial μ3-oxos. In addition to μ3-oxo, the uranyl pentagonal bipyramids are coordinated to oxygens from H_2O and acetate. In the extended

crystal structure, the **U_4Tc** clusters arrange themselves in ac plane in an alternating fashion with respect to the direction of Tc=O bond. The clusters then stack on top of each other along b axis (**Figure S3**). There is presence of isolated H_3O^+ and H_2O molecule in between the cluster which forms H-bonding with UO_2^+ and H_2O coordinated to them. The overall molecular formula of the crystalline structure of **U_4Tc** is: $[(UO_2)_4(TcO)(O)_4(CH_3COO)_4\ (H_2O)_4.\ H_3O.H_2O]$. $Tc(V)O_5$ umbrella unit has been reported before in handful studies and isolated by coordinating with catechol containing ligand[37-39]. However, the **U_4Tc** is the first evidence of $Tc(V)O_5$ umbrella coordinating with a metal center through oxo bond. The average $Tc{=}O_{ax}$ and $Tc\text{-}O_{eq}$ bond length in this study was 1.656 and 1.896, respectively. These values match very well with the previously reported $Tc(V)O_5$ (**Table S3**). The bond valence sum value for Tc(V) metal center was consistent with oxidation state with value 5.35 (**Table S2**). The $(UO_2)_4O_4$ tetramer unit present in **U_4Tc** has been utilized by Thuery and coworkers to synthesized polymetallic complexes of calixarenes[40]. But coordination of this tetramer with a transitional metal ion like Tc(V) was unknown.

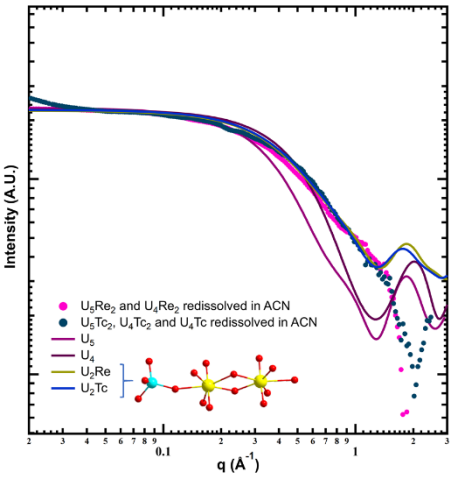

Figure 3. SAXS pattern for solution of crystalline material dissolved in acetonitrile.

The SAXS analysis on mother liquor/redissolved crystal in water didn't show presence of cluster in the solution. The species present in water were monomeric (**Figure S4**). Apart from water, the crystalline materials were only moderately soluble in acetonitrile. SAXS pattern of acetonitrile solution suggested presence of uranyl species smaller than pentamer or tetramer (**Figure 3**). The curve matches well with simulated uranyl dimer species (part of U_5/U_4) coordinated to a perrhenate/pertechnetate. This suggested dissociation of larger molecular cluster present in solid state to smaller fragments in acetonitrile.

Additional chemical characterization has been done on bulk crystalline materials obtained from reaction between uranium acetate and perrhenic acid by using Fourier Transform Infrared Spectroscopy (FTIR), Raman spectroscopy, Powder X-ray Diffraction (PXRD) and Scanning Electron Microscopy-Energy Dispersive Spectroscopy (SEM-EDS). In case of technetium containing crystalline materials, the characterization has been kept limited to Raman spectroscopy and SEM-EDS to avoid radioactive contamination. All these characterizations are representation from multiple phases present in the crystalline materials.

The FTIR spectra of crystalline materials from reaction between uranium acetate and perrhenic acid showed characteristic band for -OH stretching in between 3600-3100 cm^{-1} from H_2O and hydroxyl groups (**Figure S5**). Vibrational frequency corresponds to different group present in CH_3COO- can be found in between 1520-1420 cm^{-1} and assigned in **Table S4**. A wide peak in between 990-780 cm^{-1} corresponds to UO_2 and ReO_4 stretching. Similar to previous studies, the stretching corresponding to this two separate group in FTIR can't be distinguish from one another[4]. However, the Raman spectra (**Figure S6**) was found to be useful in distinguishing the groups. The Raman active ν_1 and ν_3 stretching of ReO_4 can be observed in 998 cm^{-1}, 946 cm^{-1} and 856 cm^{-1}.[2, 41] In case of crystalline materials from reaction between uranium acetate and pertechnic acid, this stretching shift into lower wavenumber for TcO_4^- at position 978 cm^{-1}, 908 cm^{-1} and 830 cm^{-1}.[42, 43] The Raman active ν_1 stretching of uranyl group can be also observed at 828 cm^{-1} for perrhenate compound and 820 cm^{-1} for pertechnetate compound[2, 44].

PXRD pattern of crystalline materials isolated from reaction between uranium acetate and perrhenic acid have shown peaks corresponds to **U_5Re_2** and **U_4Re_2** (**Figure S7**). However, preferred crystallographic orientation and similar position of peaks for different phases from simulated pattern made the assignment of some peaks difficult.

The SEM analysis on crystalline materials have shown block and plate shaped crystals (**Figure S8 and S9**). The EDS pattern agreed well with elucidated structures from SCXRD by showing peaks corresponding to U, Tc/Re, Na, C and O in the crystalline materials (**Figure S8 and S9**). The results of EDS semi-quantitative elemental analysis are in **Table S5 and Table S6**.

This work contributed towards understanding coordination between oxoanionic/reduced Tc-99 and UO_2^{2+} species which co-exist in spent nuclear fuel/legacy waste. The crystallization of SBU in **U_5Re_2, U_5Tc_2** and **U_4Tc** molecular cluster also supporting our previous hypothesis that perrhenate/pertechnetate can be good capping agent to isolate intermediate metal-oxo species from the solution[7]. We will extend our current work to tetravalent actinides such as U(IV), Pu(IV), etc. in the future. This study was supported by the Department of Energy, National Nuclear Security Administration under Award DE-NA0003763. Tc-99 was supplied by the U.S. Department of Energy Isotope Program, managed by the Office of Isotope R&D and Production.

Conflicts of interest

There are no conflicts to declare.

Notes and references

§ Electronic Supplementary Information (ESI) available: [CCDC 2332264-2332268] contains CIF files of structures. Additional

figures and details of synthesis and chemical characterization are available in SI.

§§ *Caution!!* Radioactive materials were used: ^{99}Tc (β-emitter) and ^{238}U (α-emitter). Experiments were conducted by trained personnel in a licensed research facility with special precautions taken towards the handling, monitoring, and disposal of radioactive materials.

1. K. George, A. J. Masters, F. R. Livens, M. J. Sarsfield, R. J. Taylor and C. A. Sharrad, *Hydrometallurgy*, 2022, **211**, 105892.
2. M. J. Sarsfield, A. D. Sutton, I. May, G. H. John, C. Sharrad and M. Helliwell, *Chemical Communications*, 2004, DOI: 10.1039/B404424J, 2320-2321.
3. A. D. Sutton, I. May, C. A. Sharrad, M. J. Sarsfield and M. Helliwell, *Dalton Transactions*, 2006, DOI: 10.1039/B611046K, 5734-5742.
4. O. V. Karimova and P. C. Burns, *Inorganic Chemistry*, 2007, **46**, 10108-10113.
5. A. M. Fedosseev, N. A. Budantseva, M. S. Grigoriev, K. E. Guerman and J.-C. Krupa, *Radiochimica Acta*, 2003, **91**, 147-152.
6. M. Shohel, J. Bustos, G. D. Stroscio, A. Sarkar and M. Nyman, *Inorganic Chemistry*, 2023, **62**, 10450-10460.
7. M. Shohel, J. Bustos, A. Roseborough and M. Nyman, *Chemistry – A European Journal*, 2023, **n/a**, e202303218.
8. M. Shohel, A. K. Sockwell, A. E. Hixon and M. Nyman, *Inorganic Chemistry*, 2024, **63**, 2044-2052.
9. T. Levitskaia, S. Bryan, S. Chatterjee, J. Crum, R. Peterson, B. Riley, J. Serne and J. H. Westsik, Jr., United States, 2016.
10. G. K. Schweitzer and L. L. Pesterfield, *The aqueous chemistry of the elements*, OUP USA, 2010.
11. S. Chatterjee, V. E. Holfeltz, G. B. Hall, I. E. Johnson, E. D. Walter, S. Lee, B. Reinhart, W. W. Lukens, N. P. Machara and T. G. Levitskaia, *Analytical Chemistry*, 2020, **92**, 13961-13970.
12. R. J. Serne, B. M. Rapko and I. L. Pegg, *Technetium Inventory, Distribution, and Speciation in Hanford Tanks*, United States, 2014.
13. G. Kickelbick, in *Hybrid Materials*, 2006, DOI: https://doi.org/10.1002/9783527610495.ch1, pp. 1-48.
14. P. Li, N. A. Vermeulen, C. D. Malliakas, D. A. Gómez-Gualdrón, A. J. Howarth, B. L. Mehdi, A. Dohnalkova, N. D. Browning, M. O'Keeffe and O. K. Farha, *Science*, 2017, **356**, 624-627.
15. S. L. Hanna and O. K. Farha, *Chemical Science*, 2023, **14**, 4219-4229.
16. M. B. Andrews and C. L. Cahill, *Chemical Reviews*, 2013, **113**, 1121-1136.
17. P. C. Burns, *The Canadian Mineralogist*, 2005, **43**, 1839-1894.
18. T. A. Kohlgruber, G. A. Senchyk, V. G. Rodriguez, S. A. Mackley, F. Dal Bo, S. M. Aksenov, J. E. S. Szymanowski, G. E. Sigmon, A. G. Oliver and P. C. Burns, *Inorganic Chemistry*, 2021, **60**, 3355-3364.
19. D. E. Felton, T. A. Kohlgruber, Z. D. Tucker, E. M. Gulotty, B. L. Ashfeld and P. C. Burns, *Crystal Growth & Design*, 2023, DOI: 10.1021/acs.cgd.3c00976.
20. N. P. Deifel, K. T. Holman and C. L. Cahill, *Chemical Communications*, 2008, DOI: 10.1039/B813819B, 6037-6038.
21. T. Loiseau, I. Mihalcea, N. Henry and C. Volkringer, *Coordination Chemistry Reviews*, 2014, **266-267**, 69-109.
22. N. P. Deifel and C. L. Cahill, *Comptes Rendus Chimie*, 2010, **13**, 747-754.
23. V. V. Gurzhiy, S. A. Kalashnikova, I. V. Kuporev and J. Plášil, *Journal*, 2021, **11**.
24. E. M. Wylie, C. M. Dawes and P. C. Burns, *Journal of Solid State Chemistry*, 2012, **196**, 482-488.
25. E. M. Villa, C. J. Marr, L. J. Jouffret, E. V. Alekseev, W. Depmeier and T. E. Albrecht-Schmitt, *Inorganic Chemistry*, 2012, **51**, 6548-6558.
26. V. Kocevski, C. A. Juillerat, E. E. Moore, H.-C. zur Loye and T. M. Besmann, *Crystal Growth & Design*, 2019, **19**, 966-975.
27. J. Ling, G. E. Sigmon, M. Ward, N. Roback and P. Carman Burns, 2010, **225**, 230-239.
28. T. Z. Forbes, V. Goss, M. Jain and P. C. Burns, *Inorganic Chemistry*, 2007, **46**, 7163-7168.
29. S. V. Krivovichev, C. L. Cahill and P. C. Burns, *Inorganic Chemistry*, 2003, **42**, 2459-2464.
30. G. Morrison, M. D. Smith and H.-C. zur Loye, *Journal of the American Chemical Society*, 2016, **138**, 7121-7129.
31. G. H. John, I. May, M. J. Sarsfield, H. M. Steele, D. Collison, M. Helliwell and J. D. McKinney, *Dalton Transactions*, 2004, DOI: 10.1039/B313045B, 734-740.
32. P. Thuéry, *Inorganic Chemistry*, 2013, **52**, 435-447.
33. A. N. Alsobrook, B. G. Hauser, J. T. Hupp, E. V. Alekseev, W. Depmeier and T. E. Albrecht-Schmitt, *Chemical Communications*, 2010, **46**, 9167-9169.
34. P. Thuéry, *European Journal of Inorganic Chemistry*, 2014, **2014**, 58-68.
35. G. Andreev, N. Budantseva, A. Levtsova, M. Sokolova and A. Fedoseev, *CrystEngComm*, 2020, **22**, 8394-8404.
36. P. Thuéry, *Crystal Growth & Design*, 2008, **8**, 4132-4143.
37. M. J. Abrams, S. K. Larsen and J. Zubieta, *Inorganic Chemistry*, 1991, **30**, 2031-2035.
38. F. D. Rochon, R. Melanson and P.-C. Kong, *Acta Crystallographica Section C*, 1992, **48**, 785-788.
39. A. Davison, B. V. DePamphilis, A. G. Jones, K. J. Franklin and C. J. L. Lock, *Inorganica Chimica Acta*, 1987, **128**, 161-167.
40. P. Thuéry and B. Masci, *Polyhedron*, 2003, **22**, 3499-3505.
41. M. C. Chakravorti, *Coordination Chemistry Reviews*, 1990, **106**, 205-225.
42. M. J. Sarsfield, A. D. Sutton, F. R. Livens, I. May and R. J. Taylor, *Acta Crystallographica Section C*, 2003, **59**, i45-i46.
43. R. H. Busey and O. L. Keller, Jr., *The Journal of Chemical Physics*, 2004, **41**, 215-225.
44. G. Lu, A. J. Haes and T. Z. Forbes, *Coordination Chemistry Reviews*, 2018, **374**, 314-344.